APPLIED AND ENVIRONMENTAL MICROBIOLOGY, May 2005, p. 2564–2575 Vol. 71, No. 5
0099-2240/05/$08.00+0 doi:10.1128/AEM.71.5.2564–2575.2005

Suppressive Subtractive Hybridization of and Differences in Gene Expression Content of Calcifying and Noncalcifying Cultures of *Emiliania huxleyi* Strain 1516

Binh Nguyen, Robert M. Bowers, Thomas M. Wahlund, and Betsy A. Read*

Department of Biological Sciences, California State University San Marcos, 333 S. Twin Oaks Valley Road, San Marcos, California 92096-0001

Received 14 July 2004/Accepted 19 November 2004

The marine coccolithophorid *Emiliania huxleyi* is a cosmopolitan alga intensely studied in relation to global carbon cycling, biogeochemistry, marine ecology, and biomineralization processes. The biomineralization capabilities of coccolithophorids have attracted the attention of scientists interested in exploiting this ability for the development of materials science and biomedical and biotechnological applications. Although it has been well documented that biomineralization in *E. huxleyi* is promoted by growth under phosphate-limited conditions, the genes and proteins that govern the processes of calcification and coccolithogenesis remain unknown. Suppressive subtractive hybridization (SSH) libraries were constructed from cultures grown in phosphate-limited and phosphate-replete media as tester and driver populations for reciprocal SSH procedures. Positive clones from each of the two libraries were randomly selected, and dot blotting was performed for the analysis of expression patterns. A total of 513 clones from the phosphate-replete library and 423 clones from the phosphate-limited library were sequenced, assembled, and compared to sequences in GenBank using BLASTX. Of the 103 differentially expressed gene fragments from the phosphate-replete library, 34% showed significant homology to other known proteins, while only 23% of the 65 differentially expressed gene fragments from the phosphate-limited library showed homology to other proteins. To further assess mRNA expression, real-time RT-PCR analysis was employed and expression profiles were generated over a 14-day time course for three clones from the phosphate-replete library and five clones from the phosphate-limited library. The fragments isolated provide the basis for future cloning of full-length genes and functional analysis.

Coccolithophorids are unicellular marine algae that produce a wide variety of highly sculpted calcium carbonate cell coverings. Calcification in some coccolithophorids occurs intracellularly and is thought to begin with the conversion of calcium and bicarbonate ions into crystals of calcium carbonate that are deposited in a defined array in association with an organic matrix (35). A coccolith vesicle developing from the Golgi apparatus provides the microenvironment that promotes the formation of the crystallographically intricate coccolith structures, which are subsequently extruded from the cell to form the coccosphere (7, 20). The coccolith vesicle fuses with the plasma membrane to release the individual coccoliths. While calcification and coccolithogenesis are presumed to occur in a genetically controlled manner, the functional significance and genetic control of these complex structures and the variation in crystal shape, orientation, order, and connectivity that occurs across species are poorly understood

The size and morphology of the calcite structures are as diverse as the coccolithophorids that produce them. Some of the calcite elements are simple rhombohedral units, while others appear as ornate oval platelets, extended spicules, or elaborate coronets. The mechanisms behind the natural nanofabrication of the highly sculpted calcium carbonate coccoliths are increasingly being investigated. Scanning electron and atomic force microscopy have defined many of the structural features of various types of coccoliths (13, 41). Ecophysiological and environmental studies have related biomineralization to nutrient status, light, cell growth and division, and the life cycle of coccolithophorids (28). Biochemical analysis has led to the isolation of several macromolecules associated with the organic matrix (5, 20, 22, 34), while more recently, expressed sequence tags (ESTs) have been used to catalog genes and proteins expressed during calcification (36, 37). Despite these efforts, our understanding of the mechanisms governing biomineralization in coccolithophorids is very limited. This limitation has historically been due to the lack of molecular and genetic approaches for addressing questions regarding the biology of these globally significant marine algae.

Emiliania huxleyi (Fig. 1) is the most prominent coccolithophorid and is rapidly gaining status as the model organism for studying the biology of these organisms. *E. huxleyi* is found throughout the world's oceans, forming massive blooms sometimes covering 100,000 square kilometers (3, 14). In the laboratory, cells can be grown in batch cultures and manipulated with ease (17, 25, 30). In addition, the genome of *E. huxleyi* strain 1516 is presently being sequenced in a collaborative effort between our laboratory and the Department of Energy. Although the amount of research on biomineralization in *E. huxleyi* is growing, research aimed at identification of genes and proteins involved in calcification is still in its infancy. To date, only one protein, designated GPA, has been implicated in the process of biomineralization in *E. huxleyi* (5). GPA, which is rich in glutamic acid, proline, and alanine, contains a Ca^{2+}

* Corresponding author. Mailing address: Department of Biological Sciences, California State University, San Marcos, 333 S. Twin Oaks Valley Rd., San Marcos, CA 92096-0001. Phone: (760) 750-4129. Fax: (760) 750-3063. E-mail: bread@csusm.edu.

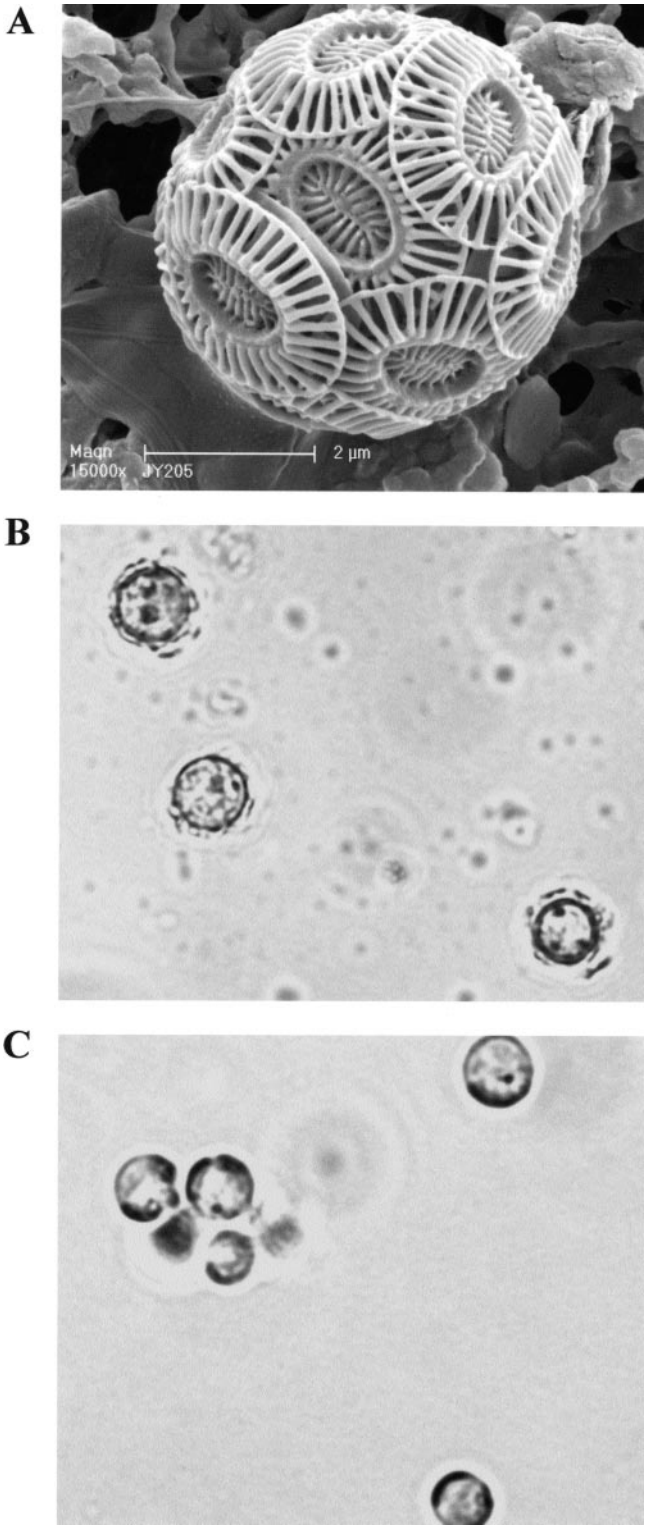

FIG. 1. (A) Scanning electron micrograph of coccolith-bearing cell of *E. huxleyi* CCMP1516 showing overlapping coccoliths (magnification, ×15,000; courtesy of J. R. Young). (B and C) Light microscopy images of CCMP 1516 cells showing (B) up-regulation of calcification in phosphate-limited (f/50) medium and (C) down-regulation in phosphate-replete (f/2) medium. Magnification, ×2,000.

motif and was isolated from intracellular polysaccharide fractions. GPA is thought to play a role in coccolith formation by controlling either crystal nucleation and growth or Ca^{2+} transport.

Until this study, biomineralization in *E. huxleyi* had only been investigated using physiological and morphological techniques, and no studies have been done employing molecular approaches for evaluating differential gene expression patterns in calcifying versus noncalcifying cells. To understand the molecular processes governing biomineralization in *E. huxleyi*, relevant subsets of differentially expressed genes must be identified, cloned, and studied in detail. In this report, we have used suppressive subtractive hybridization (SSH) to identify *E. huxleyi* genes expressed when cells are grown in phosphate-limited media, a condition known to promote biomineralization in *E. huxleyi* (1, 23, 25). SSH, developed by Diatchenko and colleagues (8), is a sophisticated technique that combines normalization and cDNA subtraction to enrich and isolate differentially expressed genes. SSH has been widely applied in plants for the identification of disease-related (6), developmentally associated (21), tissue-specific (16), and other differentially expressed genes (18, 19, 38). More recently, SSH-based methods have been employed with algae (12, 43).

There is a growing body of evidence indicating that the processes of coccolith production and calcification are closely related to phosphate metabolism in *E. huxleyi* (1, 23, 24, 32, 33). Not only are *E. huxleyi* blooms in the open ocean found predominately in oligotrophic regions, where phosphorus and nitrate are limited (32), but in the laboratory, Paasche and Bruback (24) and van Bleijswijk et al. (33) reported an increase in the ratio of carbon deposited in coccoliths to carbon incorporated in photosynthesis when cells are starved of phosphorus. Paasche (23) further demonstrated increases in the number of coccoliths and in the molar Ca^{2+}/C content of the cultures and of the coccoliths in cells grown in batch culture and/or in chemostats under phosphate-limited conditions. Andersen (1) showed that coccoltih formation could be reversibly induced in naked *E. huxleyi* cells, also known as N cells, by growing them in a phosphorus-deficient medium. While the mechanisms remain to be defined, and whether it is a direct or indirect effect remains to be determined, it is clear that phosphate limitation is linked to biomineralization and coccolith production in *E. huxleyi*.

Mutant strains that fail to calcify regardless of nutrient status are also available; however, these noncalcifying phenotypes may be caused by a point mutation in a single gene. Hence, our rationale for this study was to employ cells similar to those described by Andersen (1): cells that cease to produce coccoliths when grown under normal growth conditions and calcify when starved of phosphorus. This strategy afforded greater potential in terms of obtaining information regarding genes (and proteins) involved in coccolith production and calcification than any experimental approach previously employed. In the present investigation for SSH analysis, *E. huxleyi* strain 1516 was grown under noncalcifying conditions in phosphate-replete medium and compared to cells grown under calcifying conditions in phosphate-limited medium.

During the course of this investigation, we identified 168 gene sequences that were differentially expressed by comparing *E. huxleyi* cultures grown in phosphate-limited and phos-

TABLE 1. Oligonucleotides used for cDNA synthesis and SSH

Oligonucleotide	Sequence
SMART Oligo II	5′-AAGCAGTGGTATCAACGCAGAGTACGCGGG-3′
CDS primer	5′-AAGCAGTGGTATCAACGCAGAGTA-d(T)$_{30}$-3′
SMART PCR primer	5′-AAGCAGTGGTATCAACGCAGAGT-3′
Adapter 1	5′-CTAATACGACTCACTATAGGGCTCGAGCGGCCGCCGGGCAGGT-3′ 3′-GGCCCGTCCA-5′
PCR primer 1	5′-CTAATACGACTCACTATAGGGC-3′
Nested primer 1	5′-TCGAGCGGCCGCCCGGGCAGGT-3′
Nested primer 2R	5′-AGCGTGGTCGCGGCCGAGGT-3′

phate replete media using reciprocal SSH. Of these transcripts, 63 were specific to the phosphate-limited conditions that promote calcification, while 105 were specific to the phosphate-replete conditions that retard calcification. The differential expression pattern of a subset of these genes over a 14-day time course is discussed based on real-time RT-PCR analysis. Together, these results provide novel information for developing molecular genetic approaches for addressing important questions on the biology of coccolithophorids, including the biomineralization and coccolithogenesis processes in these organisms.

MATERIALS AND METHODS

Strains and growth conditions. *E. huxleyi* strain 1516 was obtained from the Provasoli-Guillard National Center for Culture of Marine Phytoplankton and cultured in either f/2 (phosphate replete; 41.7 μM $NaH_2PO_4 \cdot H_2O$) or f/50 (phosphate limited; 1.7 μM $NaH_2PO_4 \cdot H_2O$) artificial seawater medium as described previously (11, 17). Cells were grown in batch culture by inoculating ~5×10^7 cells into 1 liter of medium in 4-liter flasks. Cultures were grown photoautotrophically at 17 to 18°C under cool white fluorescent light (660 μmol $\cdot m^{-2} \cdot s^{-2}$) under a discontinuous light (12 h dark, 12 h light) cycle.

RNA isolation. RNA was isolated from 3 liters of late-log-phase cultures (8 days after inoculation) grown in both f/2 and f/50 cultures. Dissolution of calcium carbonate coccolith material was accomplished prior to RNA extraction by lowering the pH of the culture with HCl (0.1 N) to 5.0 for 2 min and then rapidly readjusting the pH to 8.0 with NaOH (1 N). Cultures grown in both f/2 and f/50 media were treated in this manner. A standard guanidinium isothiocyanate procedure (31) was used to isolate total RNA. Briefly, cells were lysed by grinding them in liquid nitrogen with a mortar and pestle. Membranes were further disrupted, and the activity of ribonucleases was inhibited when the cell material was resuspended in extraction buffer (4 M guanidinium isothiocyanate, 25 mM sodium citrate, 0.5% Sarkosyl, 0.1 M β-mercaptoethanol). To separate RNA from other cellular components, a phenol extraction was performed, followed by an isopropanol precipitation with 3 M sodium acetate (pH 5.2). A second precipitation using 2 M lithium chloride was carried out to further purify the RNA. The concentration and purity of the RNA concentration were determined spectrophotometrically by measuring the absorbance at 260 and 280 nm, and the integrity of the RNA was assessed using denaturing agarose gel electrophoresis.

cDNA synthesis and suppressive subtractive hybridization. Reciprocal SSH was performed by Evrogen, JSC (Moscow, Russia) using the method of Diatchenko and colleagues (8). Amplification of double-stranded cDNA was performed using 1 μg of total RNA isolated from cells grown in phosphate-replete and phosphate-limited media, using CLONTECH's SMART reverse transcriptase template-switching approach. The SMART Oligo II and CDS primers (Table 1) were used to synthesize and anchor first-strand cDNA, which was then used for PCR amplification with the SMART PCR primer (Table 1). Eighteen PCR cycles (each cycle included 95°C for 7 s, 65°C for 20 s, and 72°C for 3 min) were performed. The SMART-amplified cDNA samples were digested with RsaI to obtain shorter blunt-ended fragments for SSH procedures.

Subtractive hybridizations were performed using the SSH method in both directions (f/2 versus f/50 and f/50 versus f/2) as described previously (8, 9). For isolation of cDNAs associated with coccolith morphology, the cDNA from the phosphate-limited (f/50) *E. huxleyi* cells was used as the "tester," and the cDNA from the phosphate-replete (f/2) cells was used as the "driver." For isolation of cDNAs associated with non-coccolith-bearing morphology, the cDNA from the phosphate-replete (f/2) cells was used as the "tester," and the cDNA from the phosphate-limited (f/50) cells was used as the "driver." For each direction, two tester populations were created separately by ligating suppression adapters 1 and 2R (Table 1) to the blunt-ended RsaI-digested cDNA synthesis products. The two tester populations were mixed with 30× driver excess (driver cDNA had no adaptors) in two separate tubes, denatured, and allowed to renature. After this first hybridization, the two samples were mixed and hybridized together. The subtracted cDNA was then amplified in a primary PCR consisting of 26 cycles with primer 1 (Table 1). A secondary PCR of 11 cycles was then performed using the nested primers 1 and 2R (Table 1).

Subtracted library construction. Two subtracted cDNA samples enriched with differentially expressed sequences (f/2 specific and f/50 specific) obtained by secondary PCR were used for library construction. In each case, approximately 40 ng of purified cDNA was cloned into the pAL16 vector and used for *Escherichia coli* transformation. For both libraries, a white:blue colony ratio of 60:40 was obtained, and of the white colonies, no less than 90% contained plasmids with inserts.

Dot blot differential screening of clones. One 96-well plate of randomly picked white clones from the tester f/2-specific library and one 96-well plate of randomly picked white clones from the driver f/50-specific library were used for differential dot blot screening. The clones were grown in LB medium containing ampicillin (75 μg/ml) for 6 h at 37°C. PCR amplification of plasmid inserts was accomplished using 1 μl of culture and plasmid-specific primers. Approximately 100 ng of PCR-amplified insert DNA was arrayed in a 96-well format onto duplicated nylon membranes and hybridized with ^{32}P-labeled f/2- and f/50-subtracted cDNA probes.

Virtual Northern blots. Virtual Northern blots were prepared using 2.5 μg of SMART-amplified f/2- and f/50-unsubtracted cDNAs. The cDNA was resolved on a 1% agarose gel, processed, and blotted onto Hybond-N membranes (Roche Diagnostics, Mannheim, Germany). Individual cDNA clones generated from the SSH procedures were labeled using ^{32}P and used as probes. Membranes were hybridized and washed according to standard procedures.

DNA sequencing. The Phi29 DNA polymerase-based rolling-circle amplification method was used to prepare sequencing templates from randomly picked f/2- and f/50-specific clones. Single-pass sequencing was performed by Windsor Pond Associates (Chicago, Ill.) using the dideoxy chain termination and dye termination chemistry (Applied Biosystems). Analysis was completed on an ABI 3100 fluorescence automated sequencer.

Data handling and analysis. Expressed sequence tags from both f/2- and f/50-specific libraries were edited and assembled using the programs PHRED, CROSS_MATCH, and CONSED from PHRAP (P. Green [http://bozeman.mbt.washington.edu/]). Contaminating vector sequences were removed, and sequences having a PHRED quality score of at least 20 and a minimum size of 300 bases were taken for further analysis. Sequences from both libraries were grouped into classes of identical overlapping sequences (contigs) using PHRAP and were viewed to assess the accuracy of assembly using CONSED. For the assembly of contigs, PHRAP parameters were set at a minimum match of 20 with a default score of 30. CROSS_MATCH parameters included a minimum match of 10 and score of 20.

To identify potential homologues to the *E. huxleyi* genes, searches were performed against the nonredundant protein database in GenBank (National Center for Biotechnology Information) using BLASTX with the BLOSUM62 matrix. For all other parameters, such as filtering and word size, BLASTX default settings were employed. Similarities to known proteins were considered significant when database searches returned matches with *e* values of less than 1.0×10^{-2}.

Measuring temporal expression of select clones by real-time RT-PCR analy-

TABLE 2. Primers used for amplification of transcripts by real-time RT-PCR

Primer name	Primer sequence (5′–3′)[a]	Primer %GC	Amplicon size (bp)	Amplicon T_m[b]	
				expected	observed
F/2Contig26	For: CACCATCAATACATCGTCGGAT	45	82	78	81.5
	Rev: CTGGATCATAATCACGCACGAA	45			
F/2Contig34	For: TTTGTCGAACTTCCGCATGA	45	78	83	85.5
	Rev: TCGTTGGCGCACATACTGA	53			
F/2Contig22	For: AGGCCATCTACAACCACTACAAACC	48	77	81	83
	Rev: CCTCATGCAATTCGTGTTCCA	48			
F/50Contig29	For: AGTTGAAGTGCTGCCCTGGTT	52	97	82	85.2
	Rev: TCGTAGACAGTCCGTGGTTCCT	55			
F/50Contig31	For: CCTAGGACAGTTCATCCAAACGA	48	96	79	83.5
	Rev: GCAAAGCACAAGGACTCATCAA	45			
F/50Contig18	For: GACTTCGCCAGCTACAATCCA	52	84	81	84
	Rev: GGCGAACTTTGCCATATCCTT	48			
F/50Contig36	For: GTGTCACGCCCTCTCAATCAGT	55	76	83	85
	Rev: TGTTCGCCAGAATCGTTTCAC	48			
F/50Contig33	For: CCATCCTGCAGTCCTTGATACC	55	84	82	85.5
	Rev: AGATGCCGTTTGCGCTTT	50			

[a] For, forward; Rev, reverse.
[b] T_m, melting temperature.

sis. The mRNA expression levels of five of the f/50- and three of the f/2-specific clones were measured over a 14-day time course. Cells were grown in f/50 and f/2 media, and total RNA was extracted from cultures at 4, 7, 10, and 14 days postinoculation. First-strand cDNA synthesis was performed using an Omniscript cDNA synthesis kit (QIAGEN Inc., Valencia, CA). For cDNA synthesis, 2 μg of total RNA from each time point was used as a template in a 20-μl reaction mixture. Each reaction mixture contained 2 μg template RNA, 1× buffer reverse transcriptase (RT), 0.5 mM deoxynucleoside triphosphate, 1 μM oligo(dT) primer, 10 U of RNase inhibitor, and 4 U of Omniscript reverse transcriptase. The reaction mixture was incubated for 60 min at 37°C. cDNA was diluted 1:100, and 5 μl of the dilution was used in a SYBR Green RT-PCR.

Real-time PCR experiments were carried out using SYBER Green chemistry for amplicon detection. The SYBER Green assays were performed on the iCycler iQ System (Bio-Rad). Amplification of target genes, along with a template-minus control, was performed in triplicate in a 96-well plate. Each 25-μl reaction mixture contained 5 μl cDNA, 7.1 μl 2× SYBER Green Master Mix, and 0.24 μM (each) of forward and reverse primers. The cycling conditions for amplification included a 10-min polymerase activation at 95°C followed by 40 cycles of 95°C for 10 seconds, 60°C for 30 seconds, and 82°C for 30 seconds. Fluorescence was measured at 82°C at each cycle. The cycle threshold (C_T) value is inversely proportional to the quantity of cDNA present in the reaction mixture at that particular cycle. After PCR amplification, melt curves were generated by denaturing the sample for 1 min at 95°C, cooling it to 55°C for 1 min, and then ramping the temperature 0.5°C every 10 seconds beginning at 55°C until a final temperature of 95°C was reached. Real-time PCR data were plotted using Sigma Plot version 8.0 by taking the mean of three replicates per time point. The relative difference in expression between f/2 and f/50 cDNA clones was measured using the Basic ΔC_T method as recommended by the Bio-Rad iCycler manufacturer (Bio-Rad Laboratories). Change between f/2 and f/50 cDNA clones was calculated as $2\Delta^{CT}$. Primers were designed using Primer Express software version 1.0 (PE Applied Biosystems) and are listed in Table 2. Results from the sequence detection software were exported as tab-delimited text files and imported into Microsoft Excel for further analysis.

RESULTS

Differential screening of subtracted libraries. Figure 1 shows the effect of phosphate levels on calcification in *E. huxleyi* CCMP 1516 cells grown under phosphate-replete (f/2 medium) (Fig. 1B) versus phosphate-limited (f/50 medium) (Fig. 1C) conditions. The dramatic difference in the amount of calcification occurring in response to the phosphate concentration permitted us to employ this as a tool for looking at gene expression differences using SSH. Following construction of our reciprocal SSH libraries, dot blotting and virtual Northern blots were employed to screen the differential cDNA fragments from the two libraries (Fig. 2 and 3). Differential screen results yielded 44 f/50-specific clones (Fig. 2A) and 41 f/2-specific clones (Fig. 2B), indicating that both libraries contain about 40% positive clones. Additional clones from each of the two libraries exhibited various degrees of more subtle differential expression that may warrant further investigation. To verify differential screen results, virtual Northern blots were also performed using six of the dot blot clones from each subtracted library. Results from the virtual Northern blots are shown in Fig. 3 top (f/50-specific clones) and bottom (f/2-specific clones). Differential expression of all 12 genes from the subtracted libraries was confirmed by our virtual Northern blot results.

Sequence assembly and annotation. In order to obtain more sequence information in the form of longer reads, we sequenced and assembled several hundred clones from each library. Table 3 describes the general characteristics of the ESTs that were sequenced from each of the two SSH libraries. Of the 423 ESTs sequenced from the phosphate-limited library, 27 were singletons and the remainder were assembled into 38 contiguous sequences (contigs) with an overall EST redundancy of 93% (calculated as the number of ESTs in contigs divided by the number of ESTs). Of the 513 ESTs sequenced from the phosphate-replete library, 53 were singletons and the remainder were assembled into 50 contigs. The overall EST redundancy for the phosphate-replete library was 90%. Assembled sequences from each library were annotated by BLASTX search (e value $\leq 10^{-2}$) against the nonredundant protein database from GenBank. Overall, 23% and 34% of the identified genes from the phosphate-limited and phosphate-replete libraries, respectively, encode polypeptides with similarity to proteins with known functions in GenBank. The remaining sequences fell into the unclassified category of proteins with unknown functions (expressed as putative or hypothetical proteins) or with no GenBank match.

A complete list of the ESTs and their GenBank homologues

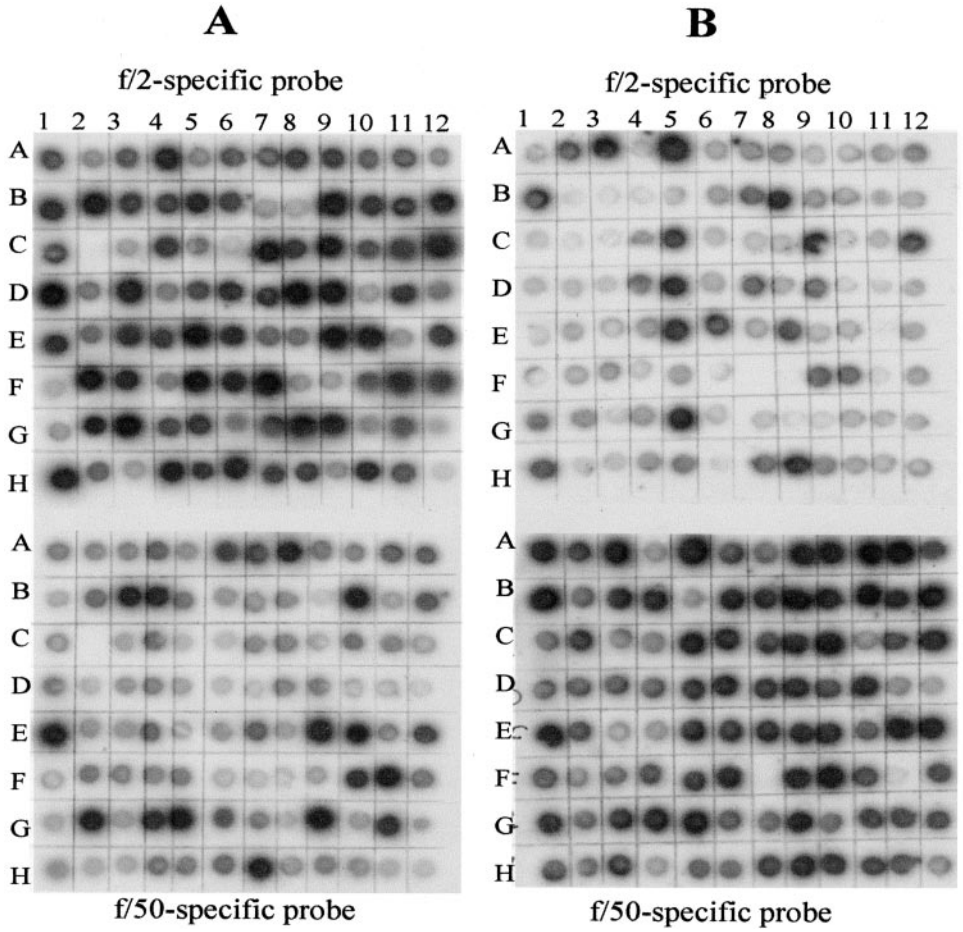

FIG. 2. Dot blot showing differential screening results of subtracted library clones from a phosphate-limited (f/50 tester) (A) and a phosphate-replete (f/2 tester) (B) plate. Clones on each plate were differentially screened with tester-specific and driver-specific cDNA probes.

for each of the SSH libraries is presented in Tables 4 and 5. The vast majority of the most abundant transcripts in the phosphate-limited data set were of unknown function, while transcripts encoding ribosomal proteins and RNA polymerase subunits were abundant in the phosphate-replete data set. Transcripts encoding proteins involved in photosynthesis, such as the photosystem I subunits and the chloroplast ATP synthase subunit proteins, were also present among the most abundant clusters in the phosphate-replete data set.

Temporal expression of selected genes by real-time RT-PCR analysis. Real-time RT-PCR was conducted to verify expression of a small subset of eight differentially expressed genes using independently prepared RNA that was extracted from cultures of f/2- and f/50-grown cells 4, 7, 10, and 14 days after inoculation. The 14-day time course was intended to determine transcripts (cDNA clones) that may be directly involved in biomineralization, as calcification is known to occur most notably during the late log and stationary phases of growth (2), which generally occur between 7 and 14 days of growth (17).

The amplification profiles (along with their respective standard deviations) and dissociation curves for each of the selected genes, three from the phosphate-replete library and five from the phosphate-limited library, are shown in Fig. 4. While contigs 18, 29, 31, and 36 from the f/50 library showed differential mRNA expression in cultures grown in phosphate-limited compared to phosphate-replete media from day 4 onward, none of the transcripts were induced immediately. Maximal differences in expression were reached 14 days following inoculation. In all cases, with the exception of contig 18, contig-specific expression was detectable under both growth conditions. By day 14, changes in gene expression for contigs 31 and 35 were 3 orders of magnitude greater for cells grown in phosphate-limited versus phosphate-replete media (Fig. 4E and G). Changes of more than 2 orders of magnitude were noted for contigs 29 and 18 at day 14 (Fig. 4D and F). Contig 18-specific expression, however, was barely detectable in cells grown in phosphate-replete medium. More modest changes in gene expression were evident for contig 33 from the f/50 library (Fig. 4H).

Real-time RT-PCR also confirmed candidates from the f/2 library whose down-regulation during phosphate limitation was revealed via SSH procedures. For example, the estimated change for contig 34 across the 14-day time course highlights the ability of SSH to identify genes that are expressed differentially, but at low levels. Down-regulation of this transcript in the phosphate-deficient cells varied between 1.5- and 3.6-fold (Fig. 4B). Transcript levels for one of the P700 reaction center proteins exhibited an interesting expression pattern across the

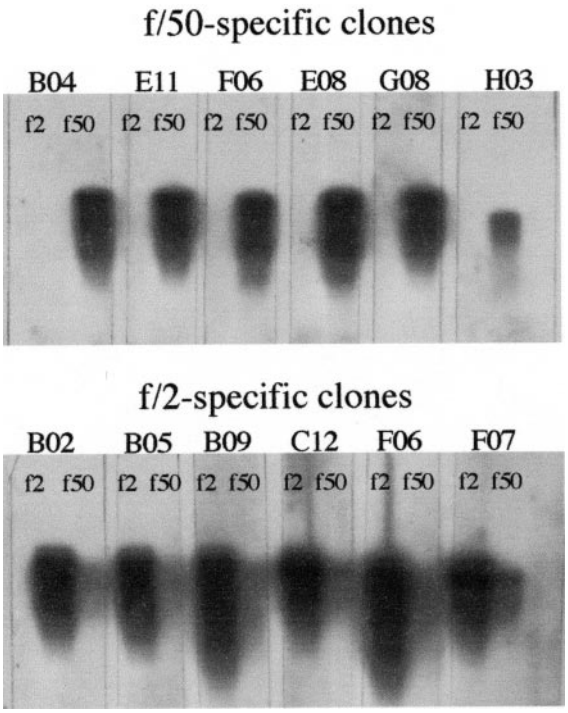

FIG. 3. Virtual Northern blot analysis of differential clones obtained from phosphate-limited (f/50) and phosphate-replete (f/2) subtracted libraries (see text for details).

14 days. The transcript was down-regulated at 4 days (~2-fold) under phosphate-limited conditions but then appeared to be up-regulated (~3- to 5-fold) during the later stages of growth (days 10 to 14) (Fig. 4A). The dissociation curves for all samples showed a single peak at the expected temperature, indicating target-specific amplification.

DISCUSSION

PCR-based suppressive subtractive hybridization was used successfully in the present investigation to detect differences in gene expression in coccolith-bearing *E. huxleyi* cells grown in phosphate-limited medium and non-coccolith-bearing cells grown in phosphate-replete medium. A total of 168 differentially expressed transcripts were identified, some of which may be related to phosphate starvation and some of which presumably are involved in calcification and coccolithogenesis. The high redundancy rates of 93% and 90% that were obtained after sequencing 423 clones from the phosphate-limited and 513 clones from the phosphate-replete libraries, respectively, may be a function of the SSH methodology. Alternatively, these rates may indicate that the potential for novel gene discovery under these conditions is nearly exhausted, suggesting that only a small number of genes, perhaps less than 100, are required for biomineralization in *E. huxleyi*.

TABLE 3. Comparative analysis of *E. huxleyi* 1516 f/2 and f/50 cDNA libraries

Descriptive category	Phosphate limited[a]	Nutrient replete[b]
No. of clones sequenced	423	513
No. of contigs	38	50
No. of singletons	27	53
No. of unigenes	65	103
No. of EST matches with *e* value of $>1 \times 10^{-2}$	37	19
No. of EST matches with *e* value of $<1 \times 10^{-2}$	15	35
No. of EST with no GenBank match[c]	13	49

[a] RNA extracted from *E. huxleyi* 1516 grown in f/50 medium (ca. 1.5 μM phosphate) as driver.
[b] RNA extracted from *E. huxleyi* 1516 grown in f/2 medium (ca. 36 μM phosphate) as driver.
[c] Searches yielding *e* values of $>10^{-2}$.

SSH is a powerful technology that enriches for differentially expressed genes, but it is by no means perfect. It is difficult to control for sequence-dependent factors, such as cDNA synthesis and PCR amplification efficiencies. Construction of leaky libraries in which the same transcript is present in the two reciprocal libraries can also be problematic. While the reciprocal libraries constructed in the present investigation were mutually exclusive, with membership in each library specific to the particular growth conditions, overrepresentation of specific clones was noted in both libraries. SSH includes a normalization step to overcome the problem of differences in mRNA abundance (8). All differentially regulated clones are expected to be equally represented after normalization. Overrepresentation of clones, such as the various ribosomal proteins, Orf122, and hypothetical protein TC0128 in the phosphate-replete library and the photosystem II reaction center protein D1, the putative senescence-associated protein, and the different hypothetical (contigs 38 and 32), unknown proteins in the phosphate-deficient library, is an artifact.

Nearly half of the clones recovered were estimated to be specific by dot blot hybridization, being either completely absent or substantially different in the two different cell types. Further tests of a smaller subset of select gene sequences using Northern blots and/or real-time RT-PCR corroborated some of the more distinctly different gene expression profiles, such as those of contigs 31 and 36 from the f/50 SSH library. Representation of quantitatively different cDNAs in the SSH libraries is also apparent, as several gene sequences present in the phosphate-replete SSH library, including the ribosomal proteins and photosynthesis transcripts, are fundamental housekeeping genes. The differential expression data of these particular genes support previous findings that suggest that calcification and coccolithogenesis are stimulated under conditions that result in reduced cell growth and increased cell size and are inhibited under conditions that favor cell growth and a decrease in cell size (4, 26, 28, 29).

The SSH method applied here has also proved to be effective in uncovering some of the distinguishing, albeit less abundant, transcripts from coccolith-bearing and non-coccolith-bearing *E. huxleyi* cells. This is evidenced by the fact that combined, 70% of the ESTs identified in this investigation (49% from the phosphate-limited and 21% from the phosphate-replete libraries) were not represented in our previously described EST data sets (36, 37) that were derived from non-normalized cDNA libraries. The effectiveness of subtraction was also demonstrated by the real-time RT-PCR data, in which the expression of eight genes tested over a 14-day time course experiment validated results obtained from these libraries. The suppressive subtraction was successful in detecting small dif-

TABLE 4. BLASTX results of most prevalent transcripts from f/2-specific SSH library[a]

SeqID	Putative ID	*e* value	Reads	Length
Sig1	Unknown	>0.001	1	865
Sig2	ORF497, homologous to *Porphyra* ORF491 (*Odontella sinensis*)	2.47E-28	1	797
Sig3	Unknown	>0.001	1	828
Sig4	Unknown	>0.001	1	543
Sig5	Unknown	>0.001	1	479
Sig6	Apocytochrome f, chloroplast precursor	7.499E-13	1	866
Sig7	RNA polymerase beta apos; apos; subunit (*Cyanidium caldarium*)	3.593E-09	1	628
Sig8	Pentose-5-phosphate-3-epimerase (*Pseudomonas fluorescens* PfO-1)	6.42E-16	1	804
Con2	Ribosomal protein S9 (*Crocosphaera watsonii* WH 8501)	1.36E-29	1	960
Con3	RNA polymerase beta prime subunit (*Gloeobacter violaceus* PCC 7421)	4.26E-38	1	913
Con4	Ribosomal protein S3 (*Nostoc punctiforme*)	1.09E-31	1	803
Con5	Ribosomal protein S3 (*Porphyra purpurea*)	3.29E-28	1	807
Con6	Ribosomal protein S3 (*Porphyra purpurea*)	1.72E-16	1	916
Con7	Unknown	>0.001	1	801
Con8	Orf122-(*Chlorobium tepidum*)	5.686E-10	1	1,002
Con9	Unknown	>0.001	2	322
Con10	Hypothetical protein (*Trichodesmium erythraeum* IMS101)	3.08E-40	2	634
Con11	Unknown	>0.001	2	433
Con12	Unknown	>0.001	2	416
Con14	Ribosomal protein S2 (*Guillardia theta*)	4.21E-24	2	863
Con15	Unknown	>0.001	2	1,174
Con16	Ribosomal protein S4 (*Nephroselmis olivacea*)	5.61E-26	2	447
Con17	Unknown	>0.001	2	419
Con18	Hypothetical protein (*Bacillus megaterium*)	8.79E-17	2	396
Con19	Unknown	>0.001	2	392
Con20	Unknown	>0.001	2	405
Con21	Unknown	>0.001	2	645
Con22	Unknown	>0.001	2	455
Con23	Signal transduction histidine kinase (*Crocosphaera watsonii* WH 8501)	1.93E-30	2	781
Con24	Unknown	>0.001	2	301
Con25	Elongation factor Tu GTP binding domain (*Bacillus anthracis* A2012)	3.32E-33	2	897
Con26	Photosystem I P700 chlorophyll *a* apoprotein A2 (*Emiliania huxleyi*)	1.76E-74	2	616
Con27	Hypothetical protein (*Plasmodium yoelii yoelii*)	5.41E-19	3	961
Con28	ATP synthase delta chain, chloroplast	1.37E-30	3	572
Con29	Unknown	>0.001	3	402
Con30	ABC transporter (*Cyanophora paradoxa*)	2.18E-49	3	621
Con31	Ribosomal protein S9 (*Crocosphaera watsonii* WH 8501)	1.18E-32	3	587
Con32	Hypothetical protein (*Nostoc* sp. strain PCC 7120)	3.50E-18	3	869
Con33	50S ribosomal protein L3 (*Prochlorococcus marinus*)	1.08E-19	3	537
Con34	Unknown	>0.001	4	1,021
Con35	Hypothetical chloroplast RF7 (*Guillardia theta*)	6.85E-04	5	364
Con36	Hypothetical protein Avar020180 (*Anabaena variabilis* ATCC 29413)	0.0001666	5	514
Con37	Preprotein translocase subunit Sec Y (*Porphyra purpurea*)	8.27E-20	6	866
Con38	COG0087: ribosomal protein L3 (*Trichodesmium erythraeum* IMS101)	1.79E-11	7	465
Con39	Chloroplast ATP synthase a chain precursor (ATPase subunit IV)	1.54E-76	7	745
Con40	Subunit epsilon of ATPase (*Ochrosphaera neapolitana*)	8.68E-30	7	1,020
Con41	Photosystem 1 subunit III (*Guillardia theta*)	1.11E-39	8	1,027
Con42	Photosystem 1 subunit XI (*Guillardia theta*)	2.82E-35	8	1,152
Con43	Predicted protein (*Methanosarcina acetivorans* strain C2A)	1.02895	10	619
Con44	Orf122 (*Chlorobium tepidum*)	8.41E-19	10	971
Con45	Ribosomal protein S2 (*Guillardia theta*)	1.41E-56	10	566
Con46	Hypothetical protein TC0128 (imported)—*Chlamydia muridarum* (strain Nigg)	0.116837	12	692
Con47	COG0092: ribosomal protein S3 (*Nostoc punctiforme*)	6.21E-31	19	651
Con48	Hypothetical protein (*Chlamydophila pneumoniae* AR39)	2.60643	56	1,570
Con49	COG0092: ribosomal protein S3 (*Anabaena variabilis* ATCC 29413)	1.27E-40	71	1,128
Con50	COG0048: ribosomal protein S12 (*Crocosphaera watsonii* WH 8501)	1.81E-37	151	1,766

[a] BLASTX results following PHRAP assembly are listed as follows: SeqID (sequence identification number) for singletons (Sig) and contigs (Con), Reads (numbers of EST fragments per assembled sequence), and Length (average sequence length in base pairs).

ferences in the expression of highly expressed, as well as less abundant, transcripts. These results demonstrate the importance of SSH-based EST sequencing as an approach complementary to existing EST resources for functional genomics research on marine coccolithophorids.

The most distinguishing feature of the SSH library prepared from the coccolith-bearing cells derived from the phosphate-limited media is the large number of transcripts that show no significant homology to sequences in GenBank. We obtained and sequenced the corresponding cDNA clones for six of the eight SSH clones that were subjected to real-time RT-PCR analysis. Since contig 26 showed significant homology to the P700 chlorophyll *a* apoprotein A2 from *E. huxleyi*, it was not characterized any further, and since contig 29 from the f/50

TABLE 5. BLASTX results of most prevalent transcripts from f/50-specific SSH library[a]

SeqID	Putative ID	*e* value	Reads	Length
Sig1	Unknown	>0.001	1	740
Sig2	Unknown	>0.001	1	1,108
Sig3	Subunit beta of ATPase (*Ochrosphaera neapolitana*)	1.93E-44	1	612
Sig4	Unknown	>0.001	1	663
Sig5	Hypothetical protein (*Plasmodium yoelii yoelii*)	1.4E-14	1	668
Sig6	Unknown	>0.001	1	781
Sig7	Unknown	>0.001	1	1,378
Sig8	Unknown	>0.001	1	537
Sig9	NADH dehydrogenase subunit 1 (*Emiliania huxleyi*)	6.56E-40	1	746
Sig10	Unknown	>0.001	1	479
Sig11	Unknown	>0.001	1	604
Sig12	Unknown	>0.001	1	721
Sig13	Unknown	>0.001	1	407
Sig14	Unknown	>0.001	1	596
Sig15	Translation elongation factor Tu (*Chromobacterium violaceum*)	1.51E-52	1	802
Sig16	Unknown	>0.001	1	790
Sig17	Unknown	>0.001	1	831
Sig18	Unknown	>0.001	1	849
Uni1	Unknown	>0.001	1	785
Uni2	Unknown	>0.001	1	893
Uni4	Unknown	>0.001	1	571
Uni5	Unknown	>0.001	1	661
Uni6	Unknown	>0.001	1	655
Uni7	347L (Invertebrate iridescent virus 6)	2.6E-07	1	559
Con8	Cytochrome *c* oxidase subunit 2 (*Emiliania huxleyi*)	8.43E-31	2	587
Con9	Unknown	>0.001	2	242
Con10	Photosystem I P700 apoprotein A2 (*Guillardia theta*)	5.21E-16	2	503
Con11	Unknown	>0.001	2	426
Con12	Unknown	>0.001	2	328
Con13	Unknown	>0.001	2	433
Con14	Unknown	>0.001	2	775
Con15	Unknown	>0.001	2	766
Con17	Unknown	>0.001	3	718
Con18	Unknown	>0.001	3	287
Con19	Unknown	>0.001	3	506
Con20	Unknown	>0.001	4	510
Con21	Unknown (*Vibrio vulnificus* CMCP6)	1.9E-05	4	509
Con22	Unknown	>0.001	4	358
Con23	Unknown	>0.001	4	528
Con24	Unknown	>0.001	5	170
Con25	Unknown	>0.001	5	348
Con26	Unknown	>0.001	8	640
Con27	Ribosomal protein S3 (*Porphyra purpurea*)	6.32E-17	8	636
Con28	Unknown	>0.001	8	596
Con29	Unknown	>0.001	16	787
Con30	Photosystem II reaction center protein D1 (*Emiliania huxleyi*)	5.39E-37	18	841
Con31	347L (Invertebrate iridescent virus 6)	4.15E-06	18	1,279
Con32	Unknown	>0.001	18	422
Con33	Hypothetical protein (*Nostoc punctiforme*)	8.19E-06	19	1,170
Con35	Putative senescence-associated protein (*Pisum sativum*)	9.65E-23	25	1,014
Con36	Unknown	>0.001	29	1,980
Con37	Unknown	>0.001	42	968
Con38	Hypothetical protein	0.00022	105	2,391

[a] BLASTX results following PHRAP assembly are listed as follows: SeqID (sequence identification number) for singletons (Sig) and contigs (Con), Reads (numbers of EST fragments per assembled sequence), and Length (average sequence length in base pairs).

SSH lacked a correlate in our previously described unigene set of 4,561 sequences from *E. huxleyi* (36), the clone and full-length sequence could not be readily obtained. In an attempt to characterize the six other sequences, we used NCBI's BLASTX and ORF-finder to identify the most likely open reading frame and employed the Protein Prediction Meta Server available through Columbia University to search for sequence motifs, domains, low-complexity regions, and protein localization signals. Secondary structure, transmembrane regions, solvent accessibility, disulfide bonds, and posttranslation modifications were also predicted.

Only a few biomineralization proteins have been identified in marine organisms. Some of these are proteins such as lustrin and perlucin from the mollusk shell; nacre and pearlin from the nacreous layer of the oyster; and MS130, SpP16, and SpP19 from the sea urchin. While these particular proteins show little sequence homology to each other or any other known biomineralization proteins (15, 27, 39), they do share a number of

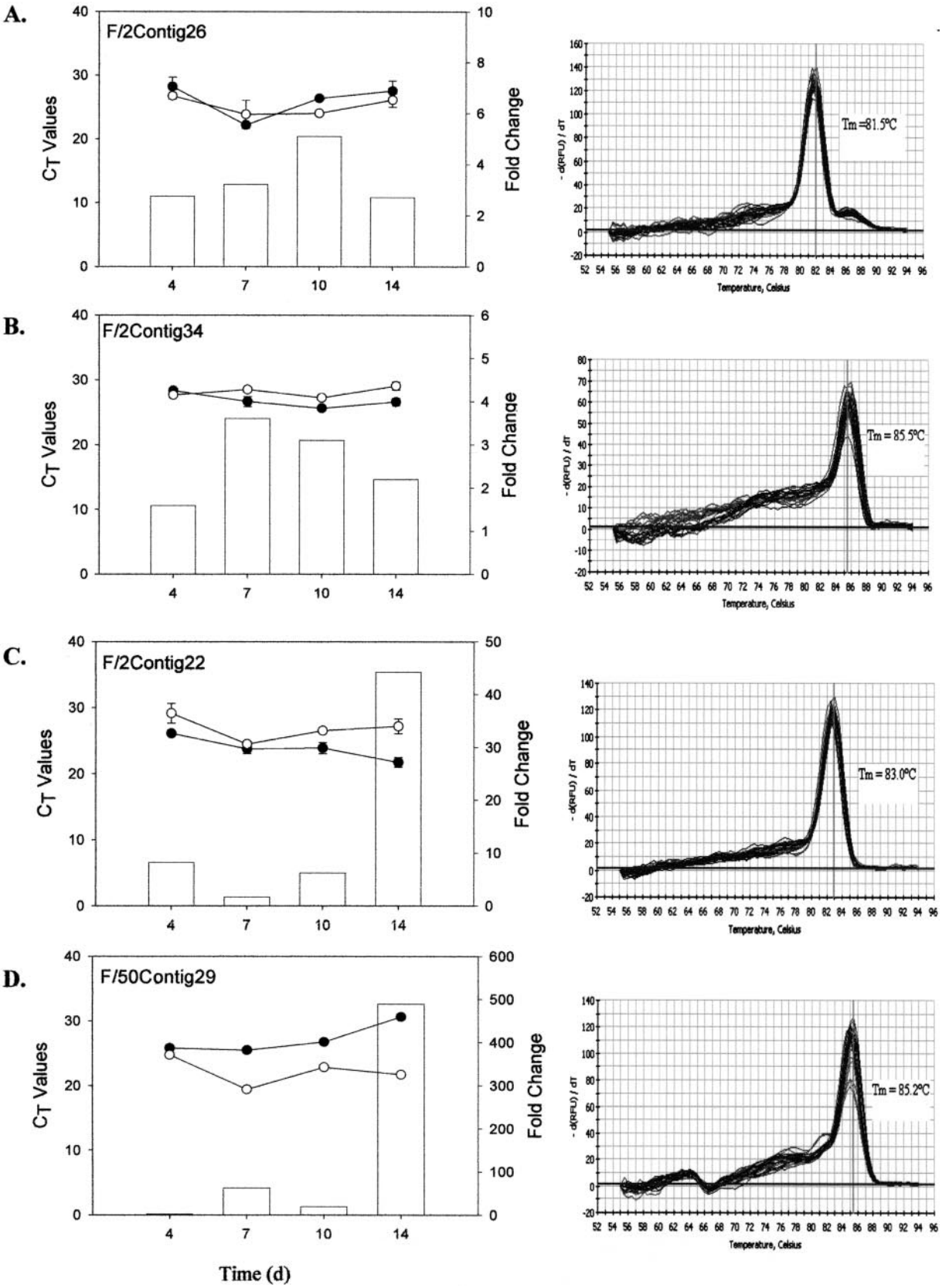

FIG. 4. Real-time RT-PCR results showing temporal expression patterns of individual cDNA transcripts from the f/2-specific (A to C) and f/50-specific (D to H) SSH libraries over a 14-day period. Total RNA was isolated from *E. huxleyi* cells grown in either f/2 (●) or f/50 (○) medium. mRNA transcript abundance is inversely proportional to the cycle threshold (C_T) value. Change (*n*-fold; bars) at each time point was calculated as $2\Delta^{Ct}$ and expressed as the relative difference in expression in f/50 versus f/2. The data represent the mean of three replicates per time point, and standard deviations are expressed as error bars. d, days.

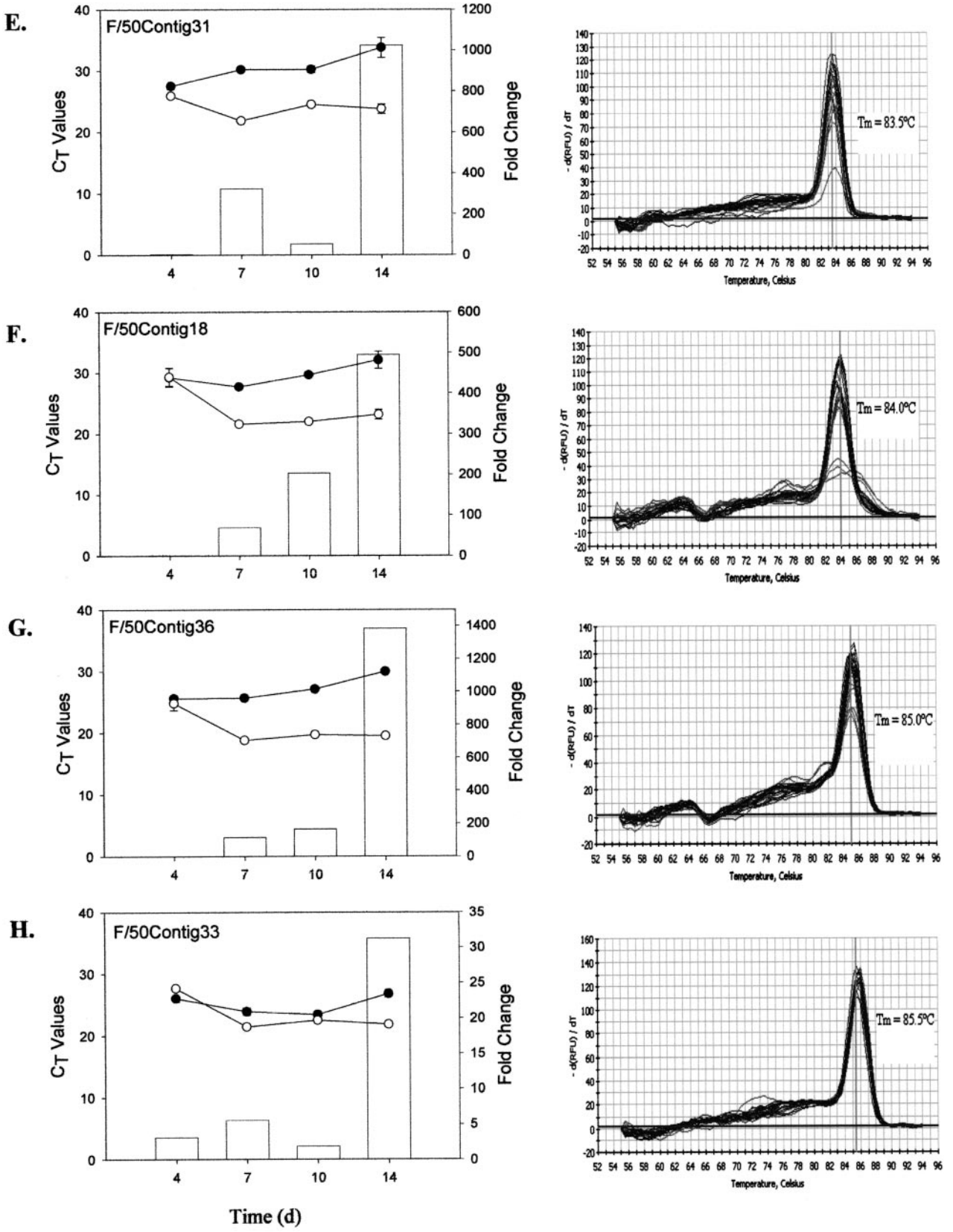

FIG. 4—*Continued*.

chemical and physical features. They generally are small acidic proteins or glycoproteins that are rich in aspartic acid or glutamic acid (10) and manifest prominent repeat sequences (40, 42). They also tend to exhibit extended or elastomeric conformations possessing little or no distinct secondary structure (42). Unfortunately, none of the gene products we examined showed homology to previously identified biomineralization proteins, nor were they noticeably acidic, nor did they contain obvious amino acid repeat elements. This result is not surprising given the limited number of biomineralization proteins identified to date and the lack of understanding of the details of the structure and function of these proteins in relation to biomineralization processes.

Contig 22 from the SSH f/2 library, which showed little differential expression until day 14, when it was up-regulated over 40-fold, exhibited no significant homology to any protein deposited in GenBank and showed no distinct motif or domain matches. The transcript is predicted to be an extracellular or cell wall protein and appears to contain three dominant alpha helices. Two of the f/50 SSH contigs that showed marked up-regulation—contig 31, which was expressed at a level 1,000-fold greater, and contig 18, which was expressed at a level 500-fold greater—in cells under phosphate-limited conditions on day 14 relative to phosphate-replete conditions also returned no significant GenBank BLASTX hits and exhibited no distinct motif or domain match. Although the cellular location of the protein correlates cannot be predicted, both proteins are expected to be membrane bound. Of the three alpha helices that can be discerned for each of the two proteins, one in contig 31 and two in contig 18 have a high probability of being transmembrane helices.

The sequences of three transcripts exhibited significant homology to proteins in GenBank. The sequence of one of the transcripts from the f/2 SSH library was up-regulated slightly (1.5- to 4-fold) across the 14-day time course in the non-coccolith-bearing cells and showed significant homology (BLASTX; 2E-07) to a hypothetical protein of unknown function from *Leptospira interrogans*. The protein, which may reside in the nucleus (PSORT), features two prominent alpha-helical regions interspersed with short stretches of beta-sheets but shows no other outstanding characteristics. The most likely protein product encoded by contig 33 from the f/50 SSH library showed significant homology to a hypothetical protein from *Nostoc* (1E-14), with more distant homology to bacterial and fungal methylase enzymes (1E-7). This particular transcript was marginally up-regulated (2- to 5-fold) in coccolith-bearing cells during the first 10 days of growth but by day 14 was significantly up-regulated (30-fold).

One of the more interesting sequences was that of contig 36 from the f/50 SSH library, which at day 14 was expressed in the phosphate-limited coccolith-bearing cells at a level that was 1,400-fold greater than in the non-coccolith-bearing cells maintained in phosphate-replete medium. The full-length sequence of the corresponding cDNA clone showed significant homology (BLASTX) to a number of ligand-gated anion channels, including that of the AVR-15 protein from *Caenorhabditis elegans* (4E-7), a glutamate-gated chloride channel from *Haemonchus contortus* (9E-06), and rat gamma-aminobutyric acid A receptor (1E-04). Four strong transmembrane helices likely to form the ion channel were predicted (using bioinformatics tools such as TMHMM, TMpred, and RPS BLAST), along with a distinct arginine-rich region outside the membrane that may represent the ligand binding domain. Our laboratory is currently trying to develop tools to determine the membrane location of the contig 36 gene product with the goal of evaluating the physiological consequences of blocking the channel or of knocking out expression of the gene to elucidate its physiological role. These data may indicate whether it is a highly selective ion channel or an indiscriminate activated channel that functions in low-affinity nutrient uptake, signaling, and/or ion transport.

The expression profiles of the phosphate-limited contigs 31, 18, 36, and 29 are intriguing, with progressively greater differential expression occurring during the later stages of growth. This is consistent with what we know about biomineralization and growth of *E. huxleyi* in batch culture (2). The effects of phosphate limitation, however, are also expected to become progressively more severe over time, and hence, we cannot unequivocally relate the differential expression patterns of these genes to biomineralization (4, 20, 27, 30).

Based upon what is presently known of biomineralization proteins, one cannot logically argue that any of the aforementioned proteins is directly involved in calcium carbonate biomineralization. However, the differential expression data support the possibility that these proteins may be peripherally involved in the processes of biomineralization and coccolithogenesis. Perhaps of greater significance is the fact that the data presented in this study provide novel and important information to the research community for developing molecular and biochemical approaches to determine the metabolic roles of these genes and gene products differentially expressed under calcifying conditions in *E. huxleyi*.

In summary, our results support the value of SSH-based EST sequencing to complement existing EST resources for functional genomics research in marine coccolithophorid algae. We have detected 168 differentially expressed transcripts in comparing coccolith-bearing and non-coccolith-bearing *E. huxleyi* cells maintained in phosphate-limited and phosphate-replete media, respectively, by screening SSH libraries. The specific expression of a subset of these genes was confirmed by a combination of dot blotting, virtual Northern blotting, and real-time RT-PCR. Given the fact that methods for genetic transformation and mutagenesis have not been developed for *E. huxleyi*, or for any coccolithophorid, additional full-length cDNA cloning, combined with more detailed functional studies using temporal cDNA microarray analysis or RNA interference methodologies, will help us to understand the molecular mechanisms underlying biomineralization and coccolithogenesis.

ACKNOWLEDGMENTS

We thank Jeremy Young (Department of Palaeontology, The Natural History Museum, London, United Kingdom) for kindly providing the scanning electron micrograph of *E. huxleyi*. We also thank Patrick Quinn for his helpful input on the manuscript.

This work was supported by a grant from the National Institutes of Health (GM 059833).

REFERENCES

1. **Andersen, O. K.** 1981. Coccolith formation and calcification in an N-cell culture of *Emiliania huxleyi* during phosphorus-limited growth in batch and chemostat cultures. Ph.D. thesis. University of Oslo, Oslo, Norway.

2. **Balch, W. M., P. M. Holligan, and K. A. Kilpatrick.** 1992. Calcification, photosynthesis and growth of the bloom-forming coccolithophore *Emiliania huxleyi*. Cont. Shelf Res. **12:**1353–1374.
3. **Brown, C. W., and J. A. Yoder.** 1994. Coccolithophorid blooms in the global ocean. J. Geophys. Res. **99:**7467–7482.
4. **Buitenhuis, E. T., H. J. W. de Baar, and M. J. W. Veldhuis.** 1999. Photosynthesis and calcification by *Emiliania huxleyi* (Prymnesiophyceae) as a function of inorganic carbon species. J. Phycol. **35:**949–959.
5. **Corstjens, P. L. A. M., A. van der Kooij, C. Linschooten, G.-J. Brouwers, P. Westbroek, and E. W. de Vrind-de Jong.** 1998. GPA, a calcium-binding protein in the coccolithophorid *Emilianis huxleyi* (Prymnesiophyceae). J. Phycol. **34:**622–630.
6. **Cramer, R. A., and C. B. Lawrence.** 2004. Identification of *Alternaria brassicicola* genes expressed in planta during pathogenesis of *Arabidopsis thaliana*. Fungal Genet. Biol. **41:**115–128.
7. **de Vrind-de Jong, E. W., and J. P. M. de Vrind.** 1997. Algal deposition of carbonates and silicates, p. 267–307. *In* J. F. Banfield and K. H. Nealson (ed.), Geomicrobiology: interactions between microbes and minerals. Mineralogical Society of America, Washington, D.C.
8. **Diatchenko, L., Y.-F. C. Lau, A. P. Campbell, A. Chenchik, F. Moqadam, B. Huang, S. Lukyanov, K. Lukyanov, N. Gurskaya, E. D. Sverdlov, and P. D. Siebert.** 1996. Suppression subtractive hybridization: a method for generating differentially regulated or tissue-specific cDNA probes and libraries. Proc. Natl. Acad. Sci. USA **93:**6025–6030.
9. **Diatchenko, L., S. Lukyanov, Y. Lau, and P. Siebert.** 1999. Suppression subtractive hybridization: a versatile method for identifying differentially expressed genes. Methods Enzymol. **303:**349–380.
10. **Gotliv, B.-A., L. Addadi, and S. Weiner.** 2003. Mollusk shell acidic proteins: in search of individual functions. Chembiochem. **4:**522–529.
11. **Guillard, R. R. L.** 1975. Culture of phytoplankton for feeding marine invertebrates, p. 29–60. *In* W. L. Smith and M. H. Chanley (ed.), Culture of marine invertebrate animals. Plenum Press, New York, N.Y.
12. **Happe, T., and A. Kaminski.** 2002. Differential regulation of the Fe-hydrogenase during anaerobic adaptation in the green alga *Chlamydomonas reinhardtii*. Eur. J. Biochem. **269:**1022–1032.
13. **Henriksen, K., S. L. S. Stipp, J. R. Young, and P. R. Bown.** 2003. Tailoring calcite: nanoscale AFM of coccolith biocrystals. Am. Mineralogist **88:**2040–2044.
14. **Holligan, P. M., E. Fernandez, J. Aiken, W. M. Balch, P. Boyd, P. H. Burkill, M. Finch, S. B. Groom, G. Malin, K. Muller, D. A. Purdie, C. Robinson, C. Trees, S. M. Turner, and P. van de Wal.** 1993. A biogeochemical study of the coccolithophore *Emiliania huxleyi* in the North Atlantic. Global Biogeochem. Cycles **7:**879–900.
15. **Illies, M. R., M. T. Peeler, A. M. Dechtiaruk, and C. A. Ettensohn.** 2002. Identification and developmental expression of new biomineralization proteins in the sea urchin *Stronglyocentrotus purpuratus*. Dev. Genes Evol. **212:**419–431.
16. **Kim, M., S. Kim, S. Kim, and B. D. Ki.** 2001. Isolation of cDNA clones differentially accumulated in the placenta of pungent pepper by suppression subtractive hybridization. Mol. Cells **11:**213–219.
17. **Laguna, R., J. Romo, B. A. Read, and T. M. Wahlund.** 2001. Induction of phase variation events in the life cycle of the marine coccolithophorid *Emiliania huxleyi*. Appl. Environ. Microbiol. **67:**3824–3831.
18. **Liao, H., F. L. Wong, T. H. Phang, M. Y. Cheung, W. Y. Li, G. Shao, X. Yan, and H. M. Lam.** 2003. GmPAP3, a novel purple acid phosphatase-like gene in soybean induced by NaCl stress but not phosphorus deficiency. Gene **318:**103–111.
19. **Mahalingam, R., A. Gomez-Buitrago, N. Eckardt, N. Shah, A. Guevara-Garcia, P. Day, R. Raina, and N. V. Fedoroff.** 2003. Characterizing the stress/defense transcriptome of *Arabidopsis*. Genome Biol. **4:**R20.
20. **Marsh, M. E.** 2003. Regulation of $CaCO_3$ formation in coccolithophores. Comp. Biochem. Physiol. **136:**743–754.
21. **Moyano, E., I. Portero-Robles, N. Medina-Escobar, V. Valpuesta, J. Munoz-Blanco, and J. L. Caballero.** 1998. A fruit-specific putative dihydroflavonol 4-reductase gene is differentially expressed in strawberry during the ripening process. Plant Physiol. **117:**711–716.
22. **Ozaki, N., S. Sakuda, and H. Nagasawa.** 2001. Isolation and some characterization of an acidic polysaccharide with anti-calcification activity from coccoliths of a marine alga, *Pleurochrysis carterae*. Biosci. Biotechnol. Biochem. **65:**2330–2333.
23. **Paasche, E.** 1998. Roles of nitrogen and phosphorus in coccolith formation in *Emiliania huxleyi* (Prymnesiophyceae). Eur. J. Phycol. **33:**33–42.
24. **Paasche, E., and S. Bruback.** 1994. Enhanced calcification in the coccolithophorid *Emiliania huxleyi* (Haptophyceae) under phosphorous limitation. Phycologia **33:**324–330.
25. **Palenik, B., and S. E. Henson.** 1997. The use of amides and other organic nitrogen sources by the phytoplankton *Emiliania huxleyi*. Limnol. Oceanogr. **42:**1544–1551.
26. **Sekino, K., and Y. Shiraiwa.** 1994. Accumulation and utilization of dissolved inorganic carbon by a marine unicellular coccolithophorid, *Emiliania huxleyi*. Plant Cell Physiol. **35:**353–361.
27. **Shen, X., A. M. Belcher, P. K. Hansma, G. D. Stucky, and D. E. Morse.** 1997. Molecular cloning and characterization of lustrin A, a matrix protein from shell and pearl nacre of *Haliotis rufescens*. J. Biol. Chem. **272:**32472–32481.
28. **Shiraiwa, Y.** 2003. Physiological regulation of carbon fixation in the photosynthesis and calcification of coccolithophorids. Comp. Biochem. Physiol. B **136:**775–783.
29. **Sikes, C. S., R. D. Roer, and K. M. Wilbur.** 1980. Photosynthesis and coccolith formation: inorganic carbon sources and net inorganic reaction deposition. Limnol. Oceanogr. **25:**248–261.
30. **Stoll, H. M., P. Ziveri, M. Geisen, I. Probert, and J. R. Young.** 2002. Potential and limitations of Sr/Ca ratios in coccolith carbonate: new perspectives from cultures and monospecific samples from sediments. Phil. Trans. Ser. A **360:**719–747.
31. **Strommer, J., R. Gregerson, and M. Vayda.** 1993. Isolation and characterization of plant mRNA, p. 49–66. *In* B. R. Glick and J. E. Thompson (ed.), Methods in plant molecular biology and biotechnology, 1st ed. CRC Press, Boca Raton, Fla.
32. **Tyrrell, T., and A. H. Taylor.** 1996. A modeling study of *Emiliania huxleyi* in the NE Atlantic. J. Mar. Syst. **9:**83–112.
33. **van Bleijswijk, J. D. L., and M. J. W. Velduis.** 1995. *In situ* gross growth rates of *Emiliania huxleyi* in enclosures with different phosphate loadings revealed by diel changes in DNA content. Mar. Ecol. Prog. Ser. **121:**271–277.
34. **Van Der Wal, P., E. W. de Jong, P. Westbroek, W. C. de Bruijin, and A. A. Muller-Stapel.** 1983. Ultrastructural polysaccharide localization in calcifying and naked cells of the coccolithophorid *Emiliania huxleyi*. Protoplasma **118:**157–168.
35. **van Emburg, P. R.** 1989. Coccolith formation in *Emiliania huxleyi*. Ph.D. thesis. Leiden University, Leiden, The Netherlands.
36. **Wahlund, T. M., A. R. Hadaegh, R. Clark, B. Nguyen, M. Fanelli, and B. A. Read.** 2004. Analysis of expressed sequence tags from calcifying cells of the marine coccolithophorid, *Emiliania huxleyi*. Mar. Biotechnol. **6:**278–290.
37. **Wahlund, T. M., X. Zhang, and B. A. Read.** 2004. EST expression profiles from calcifying and non-calcifying cultures of *Emiliania huxleyi*. J. Micropaleontol. **51:**145–155.
38. **Wang, W., P. Wu, M. Xia, Z. Wu, Q. Chen, and F. Liu.** 2002. Identification of genes enriched in rice roots of the local nitrate treatment and their expression patterns in split-root treatment. Gene **297:**93–102.
39. **Weiss, I. M., S. Kaufmann, K. Mann, and M. Fritz.** 2000. Purification and characterization of perlucin and perlustrin, two new proteins from the shell of the mollusk, *Haliotis laevigata*. Biochem. Biophys. Res. Commun. **267:**17–21.
40. **Wustman, B. A., R. Santos, B. Zhang, and S. J. Evans.** 2002. Identification of a "glycine-loop"-like coiled structure in the 34 aa pro, gly, met repeat domain of the biomineral-associated protein, PM27. Biopolymers **65:**362–372.
41. **Young, J. R., S. A. Davis, P. R. Bown, and S. Mann.** 1999. Coccolith ultrastructure and biomineralisation. J. Struct. Biol. **126:**195–215.
42. **Zhang, B., G. Xu, and J. S. Evans.** 2000. Model peptide studies of sequence repeats derived from the intracrystalline biomineralization protein, SM50. II. Pro, asn-rich tandem repeats. Biopolymers **54:**464–475.
43. **Zhang, X. N., H. Wang, Z. C. Qu, M. M. Ye, and D. L. Shen.** 2002. Cloning and prokaryotic expression of a salt-induced cDNA encoding a chloroplastic fructose-1,6-diphosphate aldolase in *Dunaliella salina* (Chlorophyta). DNA Seq. **13:**195–202.